

## Frequency pushing in lasers with injected signal

G. L. Oppo,\* A. Politi, G. L. Lippi,<sup>†</sup> and F. T. Arecchi<sup>‡</sup>

*Istituto Nazionale di Ottica, Largo Enrico Fermi 6, I-50125 Arcetri (Firenze), Italy*

(Received 14 January 1986; revised manuscript received 30 July 1986)

Suitable equations for lasers with injected signal are derived in the case of a population decay much slower than the other damping processes. A perturbative approach for a small input field  $\epsilon$  shows evidence of anomalous pushing of the laser frequency away from the external reference one. A threshold for the appearance of antisynchronized solutions is analytically found and numerically checked. A double-point bifurcation explains the switch from pulled- to pushed-frequency solutions as an exchange with a second branch of auto- $Q$ -switched periodic trajectories. The final analysis of locking threshold allows us to relate the small- and large- $\epsilon$  behavior.

### I. INTRODUCTION

Synchronization of two coupled oscillators has already a standard treatment,<sup>1</sup> whose result corresponds to a locked state with a frequency intermediate between those of the free oscillators. A class- $A$  laser<sup>2</sup> [with polarization  $\gamma_{\perp}$  and population  $\gamma_{\parallel}$  damping constants much larger than that ( $k$ ) of the field], when injected, behaves exactly in that way. As the amplitude of the external signal is increased, the frequency of the laser changes continuously from the free-case value toward the frequency of the external field.

The scenario is more complicated for class- $B$  lasers ( $k \sim \gamma_{\perp} \gg \gamma_{\parallel}$ ), since a third time constant (the frequency of the relaxed oscillations around the lasing state) enters, involving resonance phenomena. As a consequence, the frequency of the coupled system turns out to be, for some parameter values, pushed away from that of the injecting laser. A perturbative approach allows, in the small-coupling approximation, the determination of a critical pump value separating the pushing from the pulling behavior. Such a result is confirmed by numerical investigations in the strong-coupling limit as well. Moreover, numerical simulations indicate the existence of a second branch of periodic solutions corresponding to an auto- $Q$ -switched behavior<sup>2</sup> with a diverging period for vanishing external amplitudes. The two branches of limit cycles follow different routes to the locked state: While one does it through vanishing oscillation amplitudes (i.e., a reverse Hopf bifurcation, here theoretically predicted), the other shows a vanishing frequency at the critical point. The initial pushing-pulling phenomenon is shown to be related to an exchange of route between these two families of solutions in correspondence of a double-point bifurcation.<sup>3</sup> The variable position of the Hopf bifurcation on the hysteresis curve indicates the existence of a codimension-two bifurcation<sup>4</sup> where the system is marginally stable in two independent subspaces.

The paper is organized as follows. In Sec. II the model is introduced starting from the Maxwell-Bloch equations and following an improved adiabatic elimination (AE) procedure recently introduced.<sup>5</sup> Modified rate equations are obtained and the amplitude of corrections are dis-

cussed. In Sec. III a second-order application of Lindstedt-Poincaré perturbative technique is performed, yielding an expression for the frequency of the coupled system in the small external field approximation. In Sec. IV the locking region is fully analyzed by using a suitable smallness parameter. Section V is devoted to a numerical analysis of the model for different values of the external signal and of the detuning between the two lasers. In Appendix A, a perturbative analysis shows that no anomalous behavior occurs in class- $A$  lasers. Finally, in Appendix B the numerical technique used to compute periodic solutions is briefly sketched.

### II. ADIABATIC ELIMINATION

We start writing the usual set of Maxwell-Bloch equations for a single-mode, homogeneously broadened ring laser forced by an external signal with a frequency  $\omega_R$ ,

$$\begin{aligned}\dot{E} &= -k[(1+i\theta)E - P - \alpha], \\ \dot{P} &= -\gamma_{\perp}[(1+i\delta)P - E\Delta], \\ \dot{\Delta} &= -\gamma_{\parallel}[\Delta - \Delta_0 + (EP^* + E^*P)/2].\end{aligned}\tag{2.1}$$

Here,  $E$  is the complex field amplitude normalized to its saturation value,  $P$  the complex polarization,  $\Delta$  the population inversion,  $\Delta_0$  the pump rate, and  $\alpha$  the injected signal normalized as  $E$ . Moreover, having written (2.1) in a frame rotating at the external frequency  $\omega_R$ ,  $\theta$  is the cavity mistuning [ $\theta = (\omega_c - \omega_R)/k$ ,  $\omega_c$  being the cavity frequency] and  $\delta$  is the atomic detuning [ $\delta = (\omega_A - \omega_R)/\gamma_{\perp}$ ,  $\omega_A$  being the atomic transition frequency].

When the polarization (the electric field) decay rate  $\gamma_{\perp}$  ( $k$ ) is large compared to  $k$  ( $\gamma_{\perp}$ ) and  $\gamma_{\parallel}$ , the system (2.1) can be reduced to a three-dimensional flow by a simple-minded AE procedure consisting in solving the equation for the fast relaxing variable at equilibrium and introducing that value into the other equations.<sup>6</sup> Here, we operate a reduction of dimensionality based on a more accurate procedure.<sup>5</sup>

We show that if  $\gamma_{\parallel} \ll k$ ,  $\gamma_{\perp}$ , or more precisely, when

$$\mu = \left( \frac{\gamma_{\parallel}(\gamma_{\perp} + k)}{k\gamma_{\perp}} \right)^{1/2} \ll 1, \quad (2.2)$$

and for any choice of  $\tilde{\gamma} = \gamma_{\perp}/k$ , a suitable variable to be correctly eliminated always exists, namely,

$$R = (1/g\mu)(P - E), \quad (2.3)$$

where  $g = \tilde{\gamma}/(1 + \tilde{\gamma})$ . Indeed, introducing the new time scale

$$\tau = \gamma_{\parallel} t / \mu, \quad (2.4)$$

Eqs. (2.1) can be rewritten as

$$\dot{R} = -\frac{1 + \tilde{\gamma}}{\mu} \left\{ R(1/g + i\delta) - \frac{1}{g\mu} \left[ \mu w + i \left[ \frac{\theta}{\tilde{\gamma}} - \delta \right] \right] E + \frac{\alpha}{g\tilde{\gamma}\mu} \right\},$$

$$\dot{E} = R - i\theta E/g\mu + \alpha/g\mu, \quad (2.5)$$

$$\dot{w} = D - E^2 - \mu[w + g \operatorname{Re}(E^* R)],$$

where the variable  $w = (\Delta - 1)/\mu$ , and the parameter  $D = \Delta_0 - 1$  have been introduced as well. A linear stability analysis around the equilibrium values (for  $\alpha = 0$ )  $R_0 = 0$ ,  $E_0^2 = D$ ,  $w_0 = 0$ , shows<sup>5</sup> that despite the presence of two large damping constants  $k$ ,  $\gamma_{\perp}$  in Eqs. (2.1), there is only one rapidly contracting direction with a rate given by

$$\gamma_R = (1 + \tilde{\gamma})^2 / \mu \tilde{\gamma} \quad (2.6)$$

in rescaled time units. Therefore, the  $R$  variable, whose decay rate coincides with the largest negative eigenvalue  $\gamma_R$ , is well suited for being adiabatically eliminated. Incidentally, let us notice that  $\gamma_R$ , as a function of  $\tilde{\gamma}$ , has a minimum value equal to  $4/\mu$ , hence condition (2.2) guarantees the correctness of the AE of  $R$ , independently of  $\tilde{\gamma}$ . In particular, in the two limit cases  $\tilde{\gamma} \gg 1$  (CO<sub>2</sub> laser) and  $\tilde{\gamma} \ll 1$  (raser,<sup>7</sup> laser with radio wave amplification by stimulated emission of radiation), it yields the same results as for the AE of polarization and field, respectively.

At variance with Ref. 5, where the resonant case is discussed, here particular care must be taken in eliminating  $R$  because of its complex character. There are, indeed, two frequencies involved in its evolution, namely, the damping  $(1 + \tilde{\gamma})g\mu$  and the rotation  $(1 + \tilde{\gamma})\delta/\mu$ . The first of Eqs. (2.5) is of the type

$$\dot{u} = -(\gamma + i\Omega)u + v, \quad (2.7)$$

which can be formally solved as

$$u(t) = \int_{-\infty}^t \exp[-(\gamma + i\Omega)(t - \tau)] v(\tau) d\tau, \quad (2.8)$$

dropping the irrelevant dependence on the initial condition. Here the AE is a good approximation provided  $v(\tau)$  is slow compared to the rate  $\gamma + i\Omega$ . In order to minimize the rate of  $v(\tau)$ , we go to a reference frame  $\tilde{\tau}$  where the average rotational part of the motion of  $v(\tau)$  is already included. In such a new reference frame, it is then appropriate to state that

$$\frac{\dot{v}(\tilde{\tau})}{v(\tau)} \ll \gamma + i\Omega.$$

Let us go now to the laser variables. While before coupling,  $E$  rotates at a frequency  $\omega_c$  and  $P$  at rate  $\omega_A$ , after coupling the asymptotic solution both for  $E$  and  $P$  will rotate at frequency  $\omega_L$ , which has to be evaluated self-consistently. Thus  $R$  will rotate at  $\omega_L$ , and hence, in the frame rotating at  $\omega_R$ , we must introduce an extra shift  $(\omega_R - \omega_L)$ , which in scaled time units reads as

$$\beta = \left( \frac{\gamma_{\perp} + k}{\gamma_{\parallel} k \gamma_{\perp}} \right)^{1/2} (\omega_R - \omega_L). \quad (2.9a)$$

In the new reference frame,  $R$  obeys an equation like (2.5) but with  $\delta$  of the first parenthesis replaced by

$$\sigma = \delta + \frac{\beta\mu}{1 + \tilde{\gamma}}. \quad (2.9b)$$

Notice that this change would introduce a factor  $e^{-i\beta t}$  in the term, but if we represent again  $R$  in original reference frame of Eq. (2.1), the equilibrium solution is

$$R(1 + i\sigma g) = \left[ w + \frac{i}{\mu} \left[ \frac{\theta}{\tilde{\gamma}} - \delta \right] \right] E - \frac{\alpha}{\tilde{\gamma}\mu}. \quad (2.10)$$

By inspection, Eq. (2.10) could have been simply obtained by solving Eq. (2.5) with  $\dot{R} = 0$ , and at the first  $\delta$  replaced by  $\sigma$ .

We recall that relation (2.10) is valid practically for any value of  $\tilde{\gamma}$ , as for any choice of  $\theta$  and  $\delta$ . However, for simplicity, we will restrict our analysis to small detunings  $\theta$  and  $\delta$ , of order  $\mu$ . This condition is a very important one in order to have a nontrivial dynamics owing to the comparable strength of the population coupling ( $w$  term) and of the detuning effects. Substituting Eq. (2.10) into Eqs. (2.5) yields

$$\dot{E} = E \left[ w + \frac{\sigma g}{\mu} \left[ \frac{\theta}{\tilde{\gamma}} - \delta \right] \right] - iE \left[ \frac{\theta + \delta}{\mu} + w\sigma g \right] + \frac{\alpha}{\mu} \left[ 1 + \frac{i\delta g}{\tilde{\gamma}} \right], \quad (2.11)$$

$$\dot{w} = D - E^2 - \mu w(1 + gE^2) + \frac{\alpha}{2(1 + \tilde{\gamma})} (E + E^*),$$

where  $\mu^2$  terms have been neglected. In this set of equations, we recognize zero-order terms corresponding to a reversible mode<sup>8</sup> plus many corrections of first order in  $\mu$ . Let us analyze them in detail. The term with  $\mu w$  in the  $\dot{w}$  equation is the only unavoidable correction since it introduces losses in a system otherwise conservative in large-parameter regions.<sup>8</sup> All the other terms are not structurally relevant: The first one in the  $E$  equation is a constant correction to the growth rate  $w$ , the second one slightly modifies the rotating part, while the last one changes only the normalization factor for the external field. The last term in the right-hand side of the  $\dot{w}$  equation, though, compared with  $D - E^2$  is generally negligible. However, it is important to notice that all these corrections become relevant for large values of  $w$  and  $E$ , thus offering the op-

portunity for an *a posteriori* check of the correctness of the AE.

Summarizing, the relevant corrections to the naive approach (especially, for the case of CO<sub>2</sub> lasers where  $\tilde{\gamma}$  can vary from three to ten partly come from the multiplicative factor  $g$  of  $E$  in the  $w$  equation, and partly are hidden in the time scale adopted here [see Eq. (2.4)]. The final form of the equations is

$$\begin{aligned}\dot{E} &= Ew - i\eta E + \varepsilon, \\ \dot{w} &= D - E^2 - \mu w(1 + gE^2),\end{aligned}\quad (2.12)$$

where  $\eta = (\theta + \delta)/\mu$  and  $\varepsilon = \alpha/\mu$ . Section III is devoted to a perturbative analysis of these equations.

### III. SMALL EXTERNAL FIELD CASE

Equations (2.12) can be rewritten, separating the field variable  $E$  into its amplitude  $r$  and phase  $\phi$  with respect to the external field, as

$$\begin{aligned}\dot{r} &= wr + \varepsilon \cos\phi, \\ \dot{\phi} &= -\eta - (\varepsilon/r)\sin\phi, \\ \dot{w} &= D - r^2 - \mu(1 + gr^2)w.\end{aligned}\quad (3.1)$$

These equations allow an intuitive picture of the underlying dynamics: The existence of the external field induces a nonlinear coupling between a damped Toda oscillator ( $r, w$ ) (Ref. 9) and a rotator ( $\phi$ ) with constant action.

A perturbative analysis of Eqs. (3.1) for small- $\varepsilon$  values reveals the existence of a family of solutions whose frequency is pushed away from the injected one. This antisynchronization effect can be explained as a simple resonance between the rotator and the damped Toda oscillator.

In order to take into account the frequency variation of the perturbed solutions, a Lindstedt-Poincaré technique is performed for small injected amplitude  $\varepsilon$ . More precisely, we write

$$\begin{aligned}r(\tau) &= r_0(\tau) + \varepsilon r_1(\tau) + \varepsilon^2 r_2(\tau) + \dots, \\ \phi(\tau) &= (\beta_0 + \varepsilon\beta_1 + \varepsilon^2\beta_2)\tau \pm \psi_0(\tau) + \varepsilon\psi_1(\tau) \\ &\quad + \varepsilon^2\psi_2(\tau) + \dots, \\ w(\tau) &= w_0(\tau) + \varepsilon w_1(\tau) + \varepsilon^2 w_2(\tau) + \dots,\end{aligned}\quad (3.2)$$

where the expansion of  $\beta$  [Eq. (2.9a)] is introduced in order to eliminate mixed secular terms. In the zeroth order, a damped Toda equation is recovered, and the stationary solution of the unperturbed laser obtained,

$$r_0 = \sqrt{D}, \quad \beta_0 = -\eta, \quad w_0 = \psi_0 = 0, \quad (3.3)$$

where the laser frequency  $\eta$  is given by the usual pulling condition.

Knowledge of the zeroth order allows the immediate integration of the phase equation [second one of (3.1)]

$$\psi_1(\tau) = -\frac{1}{\eta\sqrt{D}}\cos(\eta\tau), \quad \beta_1 = 0, \quad (3.4)$$

showing that no first-order corrections to the average laser frequency exist. Some algebraic manipulations on

the remaining two equations yields the following linear differential equation for  $r_1$ :

$$\ddot{r}_1 + \mu(1 + gD)\dot{r}_1 + 2Dr_1 = -\eta\sin(\eta\tau) + \mu(1 + gD)\cos(\eta\tau). \quad (3.5)$$

This is the equation of a damped oscillator of frequency  $\sqrt{2D}$  (the same of the laser without injection<sup>2</sup>) externally forced with a frequency  $\eta$  (the normalized detuning). With  $\mu$  being small, the resulting motion is underdamped with a resonance at

$$\omega_0 - \omega_R = \left[ \frac{2D\gamma_{||}\gamma_{\perp}}{k + \gamma_{\perp}} \right]^{1/2}, \quad (3.6)$$

where  $\omega_0$  is the explicit frequency of the unperturbed laser, thus far hidden in  $\eta$ . The asymptotic solution of Eq. (3.5) has the form

$$r_1(\tau) = a\sin(\eta\tau) + b\cos(\eta\tau), \quad (3.7)$$

where

$$\begin{aligned}a &= \frac{\eta}{Q}[\eta^2 - 2D + \mu^2(1 + gD)^2], \quad b = 2\mu\frac{D}{Q}(1 + gD), \\ Q &= (2D - \eta^2)^2 + \mu^2\eta^2(1 + gD)^2.\end{aligned}$$

Now we can evaluate the second-order corrections, by using the first-order ones. In particular, the solution of the phase equation yields

$$\beta_2 = (2D - \eta^2)/\eta Q, \quad (3.8a)$$

$$\psi_2 = \frac{1}{4D\eta} \left[ a + \frac{1}{\eta} \right] \sin(2\eta\tau) + b\cos(2\eta\tau). \quad (3.8b)$$

Expression (3.8a) indicates that the laser frequency  $\omega_L$  is pushed away from the external one when the condition

$$\eta > \sqrt{2D} \quad (3.9)$$

is satisfied. The critical  $\eta$  value, separating the two different behaviors, coincides with the resonant one [see Eq. (3.6)], thus showing the relation of this phenomenon with the oscillatory behavior of the unperturbed laser. Indeed, such an anomalous behavior does not occur for class-A lasers (see Appendix A).

It is important to notice that in the neighborhood of the resonant point, the expansions (3.2) becomes singular. In fact, when

$$|2D - \eta^2| = O(\mu), \quad (3.10)$$

with  $\mu \ll 1$ ,  $r_1(\tau)$  diverges as  $\mu^{-1}$  and the expansion (3.2) becomes nonuniform. Nevertheless this does not affect the qualitative agreement between numerical simulations and the previous results (3.8) and (3.9). Indeed, as shown in Fig. 2, the behavior in the singular interval (3.10) follows smoothly the overall shape obtained by expansion (3.2).

### IV. LOCKING REGION

At variance with Sec. III, where small external fields were considered, here we investigate the locking region where  $\varepsilon$  can no longer be considered a small parameter.

While only a qualitative analysis was performed in Ref. 2(b) (for slightly different equations), here, exploiting the smallness of  $\mu$ , we are able to obtain exact results in a perturbative way. After a preliminary evaluation of the steady-state solutions, we present a detailed linear stability analysis, showing the existence of a codimension-two bifurcation.

Let us start with the zeroth-order approximation ( $\mu=0$ ) of Eqs. (3.1). The stationary solutions are given by

$$I=D, \quad w=\pm(A/I-\eta^2)^{1/2}, \quad A>D\eta^2 \quad (4.1)$$

where  $I=r^2$  is the output intensity, and  $A=\varepsilon^2$  the input one. As it is easily seen, the lower branch of the original hysteresis cycle is lost, while the middle and upper ones collapse [in the  $(A,I)$  plane] onto the half line  $I=D$  (see Fig. 1). The degeneracy is, however, only apparent, since different  $w$  values (opposite in sign) are associated with the same intensity  $I$ . Therefore, for  $A=D\eta^2$  a tangent bifurcation occurs, and, as a second step, we are interested in evaluating the corrections due to a finite  $\mu$ . The general solution of Eqs. (3.1) is given by the implicit relations

$$A=I(w^2+\eta^2), \quad w=\frac{(D-I)}{\mu(1+gI)}, \quad (4.2)$$

well approximated by a narrow parabola whose equation can be evaluated by substituting the second of Eqs. (4.2) into the first one, and replacing  $I$  with  $D$  everywhere except for the  $(D-I)$  term as follows:

$$A=D\eta^2+\eta^2(I-D)+D(I-D)^2/(1+gD)^2\mu^2. \quad (4.3)$$

Therefore, the coordinates of its vertex, correct up to order  $\mu^2$ , are straightforwardly given by

$$I_V=D-\frac{\mu^2\eta^2}{2D}(1+gD)^2, \quad (4.4)$$

$$A_V=D\eta^2-\frac{\mu^2\eta^2}{4D}(1+gD)^2.$$

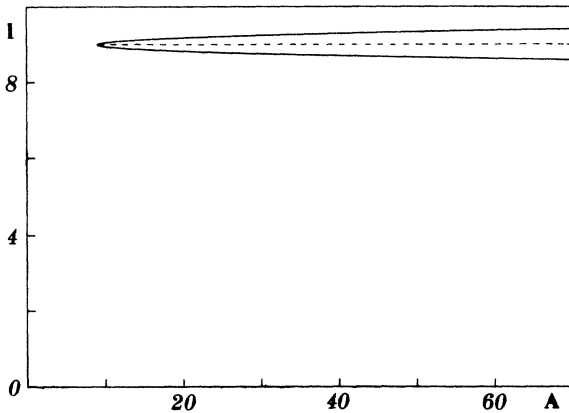


FIG. 1. Stationary-state diagram of laser with injected signal. The output intensity  $I$  is plotted vs the input one  $A$  for  $D=9$ ,  $\mu=1.58\times 10^{-2}$ , and  $\eta=1$  [see Eqs. (4.2)]. Lower branch, being very close to  $A$  axis, cannot be located. Parabolic approximation (4.3) of middle and upper branch is almost indistinguishable from the exact result in this parameter range. Hatched straight line represents the degenerate case  $\mu=0$ .

To investigate the local stability, we rewrite Eqs. (3.1) using Cartesian, instead of cylindrical, coordinates

$$\begin{aligned} \dot{x} &= wx + \eta y + \varepsilon, \\ \dot{y} &= wy - \eta x, \\ \dot{w} &= D - \mu w - (x^2 + y^2)(1 + \mu gw), \end{aligned} \quad (4.5)$$

and, linearize around a generic fixed point  $x_0, y_0, w_0$ . The associated characteristic polynomial

$$\begin{aligned} \lambda^3 + \lambda^2[\mu(1+gI_0) - 2w_0] \\ + \lambda[w_0^2 - 2w_0\mu(1+gI_0) + 2I_0(1+\mu gw_0) + \eta^2] \\ + w_0^2\mu(1+gI_0) - 2I_0w_0(1+\mu gw_0) + \eta^2\mu(1+gI_0) \end{aligned} \quad (4.6)$$

reduces, in the limit case  $\mu=0$ , to

$$\lambda^3 - 2w_0\lambda^2 + \lambda(w_0^2 + 2I_0 + \eta^2) - 2I_0w_0 = 0. \quad (4.7)$$

Therefore, imposing  $w_0=0$  (the value corresponding to the tangent bifurcation) we have

$$\lambda(\lambda^2 + 2I + \eta^2) = 0. \quad (4.8)$$

We notice that, besides the expected  $\lambda=0$  solution, a pair of purely imaginary solutions  $\lambda=\pm i(2D+\eta^2)^{1/2}$ , is present, showing the existence of a codimension-two bifurcation. The superposition of tangent and Hopf bifurcations persists independently of  $D$  and  $\eta$  values, owed to the reversible structure of the flow for  $\mu=0$  (see Ref. 8 for a detailed discussion on a generic two-dimensional reversible flow). However, a finite  $\mu$  destroys the degeneracy and a codimension-two bifurcation is expected only on a critical line in the  $(D,\eta)$  plane. Having already computed the corrections to the tangent bifurcation value [see Eq. (4.4)], we now turn our attention to the Hopf one.

The condition for the Hopf bifurcation is easily derived recalling that, whenever a real solution  $-a$  coexists with a pair of imaginary solutions  $+i\sqrt{b}$ , the characteristic polynomial has to be written as

$$\lambda^3 + a\lambda^2 + b\lambda + ab = 0. \quad (4.9)$$

Hence, we have to impose that the  $\lambda^0$  coefficient be equal to the product of  $\lambda^1$  and  $\lambda^2$  coefficients. By assuming  $\mu^2$  corrections to the zeroth-order estimate  $I=D$  (i.e.,  $w_H$  of order  $\mu$ ), and neglecting higher-order terms in Eq. (4.7), the condition reads as

$$\begin{aligned} [\mu(1+gI_H) - 2w_H](2I_H + \eta^2) = -2I_Hw_H \\ + \eta^2\mu(1+gI_H), \end{aligned} \quad (4.10)$$

whose solution yields

$$I_H = D - \frac{D\mu^2(1+gD)^2}{D + \eta^2}. \quad (4.11)$$

By comparing Eq. (4.11) with the first of (4.4) we have

$$I_H = I_V + \frac{\mu^2(1+gD)^2(\eta^2 + 2D)(\eta^2 - D)}{D + \eta^2}, \quad (4.12)$$

which shows the existence of a codimension-two bifurcation for

$$\eta^2 = D. \quad (4.13)$$

In other words, for  $\eta < \sqrt{D}$  ( $> \sqrt{D}$ ), the Hopf bifurcation occurs in the unstable, middle (stable, upper) branch. A more detailed analysis of the bifurcation unfolding requires formal tools as the normal forms, hence it goes beyond the aims of the present paper, and is left to a future work.

Finally, coming back to the frequency  $(\eta^2 + 2D)^{1/2}$  of the oscillations, we see that it is larger than the free laser frequency  $\eta$ , thus indicating the possible extension of the pushing phenomenon, so far predicted in the limit of small  $\epsilon$ 's by Eq. (3.8), to large external fields. It is sufficient that, increasing  $\epsilon$ , the free laser trajectories are deformed with continuity until the locking is reached via a reverse Hopf bifurcation. However, the persistence of the Hopf bifurcation even for  $\epsilon$  values smaller than  $\sqrt{2D}$  seems to suggest that, after an initial pulling-pushing behavior, pushing always prevails at large  $\epsilon$ 's. But this is in contrast with the standard results on locking mechanisms for class-*A* lasers where a divergence of the period is observed. As a consequence, a second family of solutions can be reasonably guessed, and a detailed two-parameter numerical investigation is needed to get a global picture of the bifurcation diagram.

## V. NUMERICAL RESULTS

In this section we present a numerical investigation of Eqs. (3.1) for different  $\eta$  and  $\epsilon$  values, and for fixed values of pump ( $D=9$ ) and damping ( $\mu=1.58 \times 10^{-2}$ ). The periodic solutions have been evaluated by means of a Newton's method on a suitable Poincaré section (see Appendix B for a brief discussion of its application).

We start checking the existence of the resonance around  $\eta = \sqrt{2D}$ . In order to keep track of effects due to the locking on a stationary state, we perform our calculations along the straight lines

$$\eta = m\epsilon \quad (5.1)$$

in the parameter space  $(\eta, \epsilon)$ , thus rescaling the  $\epsilon$  interval of unlocked states to  $(0, \infty)$  independently of  $\eta$ . Since small  $\epsilon$ 's correspond to large angular coefficients  $m$ , we have performed a numerical analysis for  $m=35, 25, 20$ , and  $15$  (curves *a, b, c*, and *d*, respectively, in Fig. 2). The agreement with the theoretical results [Eq. (3.8a)] is quite good for  $m=35$ , while increasing the external field has the double effect of decreasing the resonance frequency and introducing hysteresis phenomena.

In Fig. 3 we have reported the laser frequency versus  $\epsilon$ , for fixed  $\eta$ , in order to better investigate the effect of large injection amplitudes. The first evident result in the persistence of the pushing phenomenon even for large values as inferred in Sec. IV, with the only difference that the threshold between the two distinct behaviors does not coincide with the perturbative estimate  $\sqrt{2D}$ . In fact, looking at the curve of Fig. 3 corresponding to  $\eta=3.9 < \sqrt{2D}=4.24 \dots$ , we notice that, after an initial frequency decrease, the anomalous asymptotic growth sets in. The discontinuous switch from one behavior to the other again suggests the existence of a second family of

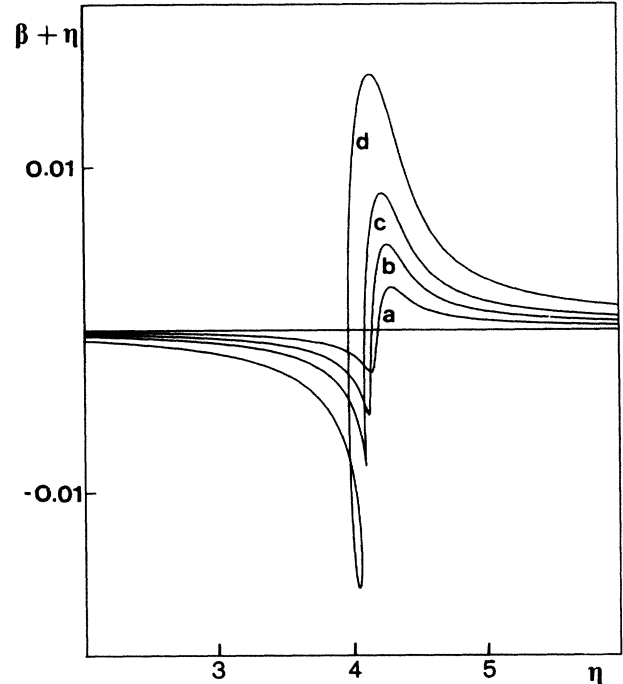


FIG. 2. Frequency difference between injected ( $\beta$ ) and free ( $-\eta$ ) laser case vs detuning  $\eta$  for fixed  $m(=\eta/\epsilon)$  values. Curves *a, b, c*, and *d* correspond to  $m=35, 25, 20$ , and  $15$ , respectively.

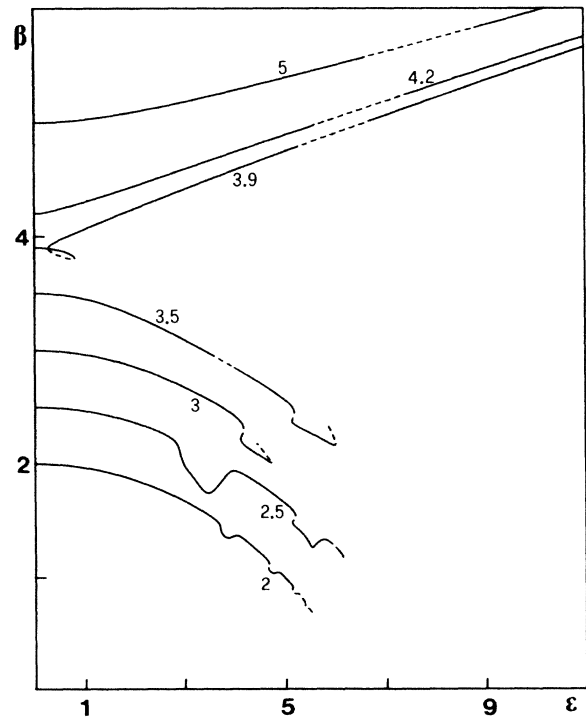


FIG. 3. Laser frequency  $\beta$  vs external amplitude  $\epsilon$ , for fixed detuning values. Reported numbers indicate the respective  $\eta$  values. Hatched segments stand for unstable solutions.

solutions which has been, indeed, found. It corresponds, for decreasing  $\epsilon$  values, to short pulses separated by a divergent period. Their frequency behavior is sketched in Fig. 4 where the different curves (corresponding to the same  $\eta$  values as in Fig. 3) for clarity. A picture complementary to that shown in Fig. 3 emerges. In fact, for any  $\eta$  value the curves of the two different families show opposite asymptotic behaviors: One reaches the locking through a frequency decrease, while the other through an amplitude decrease. This last route, which cannot be inferred from Figs. 3 and 4, corresponds in practice to a frequency increase up to a maximum value at the bifurcation point. In Fig. 4 the four high branches ( $\eta=2$  to 3.5) end at the Hopf bifurcation.<sup>10</sup> For each of these curves the oscillation amplitude increases with the square root of the separation of  $\epsilon$  from its critical value. This was checked in the numerical solutions. In Fig. 3 the three upward branches ( $\eta=3.9$  to 5) end also into Hopf points which are located outside the figure edge.

A comparison of Figs. 3 and 4 thus suggests an exchange between the two different small- $\epsilon$  behaviors with the two asymptotic ones. In Fig. 5, where both cases have been drawn in an enlarged picture, the existence of an exchange mechanism is already transparent. The further specialized analysis gives evidence of a double-point bifurcation for  $\eta=3.853\dots$  (see Fig. 6). As a consequence we

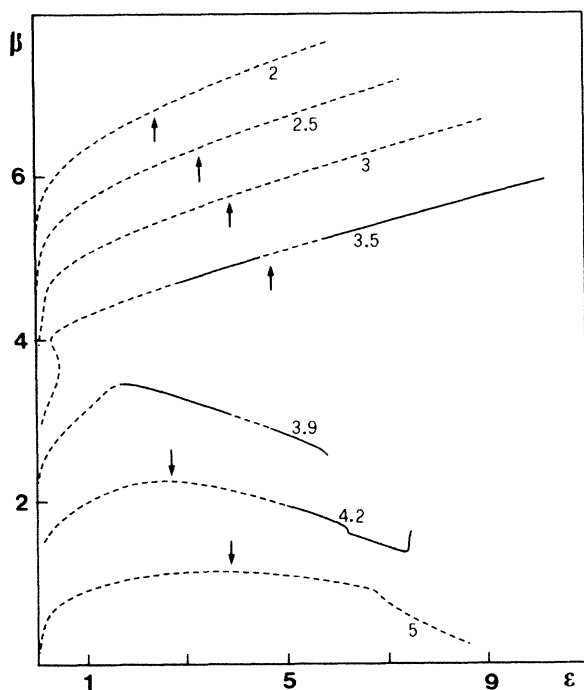


FIG. 4. Second family of periodic solutions. The laser frequency  $\beta$  is plotted vs the external amplitude  $\epsilon$  for fixed  $\eta$ . Detuning values have been chosen equal to those in Fig. 3. Starting from above, curves have been vertically shifted by increments of 3.0, 2.3, 1.5, 0.5, 0,  $-1.0$ , and  $-2.0$ , respectively, to prevent a confusing superposition. Hatched segments indicate unstable solutions.

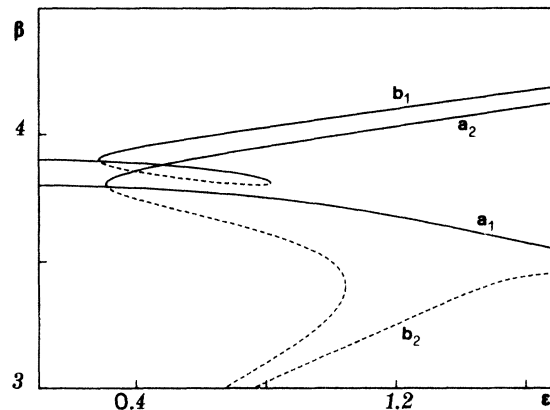


FIG. 5. Laser frequency  $\beta$  vs external amplitude  $\epsilon$  for  $\eta=3.8$  (curves  $a_1, a_2$ ), and  $\eta=3.9$  (curves  $b_1, b_2$ ), below and above the double-point bifurcation, respectively. Subscript  $j$  indicates whether the branch belongs to the first ( $j=1$ ), or to the second ( $j=2$ ) family of solutions.

notice that two distinct thresholds exist for the pushing-pulling phenomenon: a “local” one referring to the small- $\epsilon$  region, and a “global” one corresponding to an exchange between the different branches.

We end this section with a few comments on the asymptotic behavior of the different cases of solutions. Looking at Figs. 3 and 4 none of the decreasing curves are terminated. This is due either to increasing difficulties dealing with larger periods ( $\eta=2.0$  and  $2.5$  in Fig. 3), or to the existence of a reverse period-doubling bifurcation ( $\eta=3.0$  and  $3.5$  in Fig. 3) where the branch ends up collapsing on the corresponding branch denoted by the same symbol in Fig. 4. However, according to a second double-point bifurcation, the families corresponding to  $\eta=3.0$  and  $3.5$  are exchanged with a third branch (not displayed in Figs. 3 and 4) which still reaches the locking through a diverging period route.

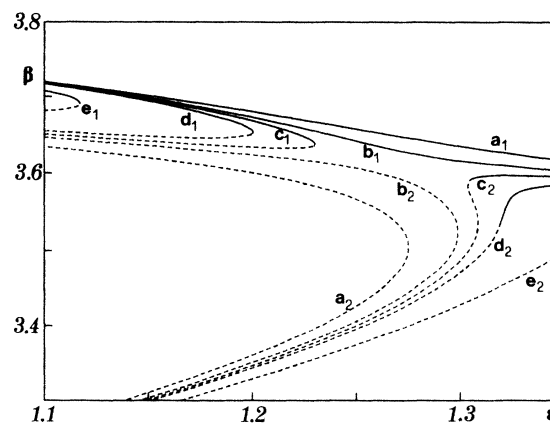


FIG. 6. Laser frequency  $\beta$  vs external amplitude  $\epsilon$  for five  $\eta$  values close to the double-point bifurcation  $\eta=3.853$ . Letters  $a$ ,  $b$ ,  $c$ ,  $d$ , and  $e$  refer to  $\eta=3.85$ ,  $3.853$ ,  $3.854$ ,  $3.855$ , and  $3.86$ , respectively. Subscript numbers have the same meaning as in Fig. 5.

## VI. CONCLUSION

An improved method of adiabatic elimination has yielded a modified set of equations for a class-*B* laser with an injected signal. An anomalous pushing behavior of the laser frequency has been evidenced through a second-order perturbative technique and confirmed by a numerical analysis which has also clarified the relations between the small behavior and large phenomena around the locking region. A codimension-two bifurcation naturally follows from the competition between the normal pulling and the anomalous pushing phenomenon.

Numerical evidence of a frequency-pushing phenomenon was already given by Gu *et al.*<sup>11</sup> in a parameter range far away from that explored here. Indeed, they use a pump parameter  $D = 39$  and  $\mu = 0.41$  which does not make our perturbation expansion fully applicable. However, we can notice that their single choice of  $\eta$  ( $=2.44$ ), being much smaller than the critical value  $\sqrt{2D} = 8.8$ , yields a small- $\epsilon$  pulling behavior according to our Eq. (3.8a).

## ACKNOWLEDGMENTS

We acknowledge financial support from the European Economic Community [Contract No. STI 082 JC (CD)]. We wish to thank J. Tredicce, G. P. Puccioni, A. Poggi, E. Celarier, and N. B. Abraham for useful discussions. Two of us (G.L.O. and A.P.) are grateful to Professor R. Kapral for his warm hospitality and kind interest.

## APPENDIX A

The pushing effect discussed in Sec. III appears to be strictly related to the existence of damped oscillations in the unforced laser. In fact, we show in this appendix that such a phenomenon does not exist in class-*A* lasers ( $\gamma_{\perp}, \gamma_{\parallel} \gg k$ ). After the AE of both polarization and population inversion, the equations are

$$\begin{aligned} \dot{r} &= -r + \Delta_0 r / (1 + r^2) + \alpha \cos \phi, \\ \dot{\phi} &= -\eta - (\alpha/r) \sin \phi, \end{aligned} \quad (\text{A1})$$

where the time scale is normalized to  $k$ . These equations were given by Spencer and Lamb<sup>12</sup> and analyzed by Yamada and Graham<sup>13</sup> in the case of modulated external amplitude.

An application of the perturbative expansion of Sec. III leads, with the obvious meaning of symbols, to

$$\dot{r}_1 = -2Dr / (1 + D) + \cos(\eta t), \quad (\text{A2})$$

$$\beta_2 = -2D / [4D^2 + \eta^2(1 + D)^2]. \quad (\text{A3})$$

Expression (A2) shows an exponential decay towards the asymptotic oscillation of frequency  $\eta$ , without any resonance phenomena. As a consequence, the second-order correction  $\beta_2$  to the laser frequency does not change sign and hence no antisynchronized effects are possible. Let us recall that the second-order dependence of the laser frequency from the external amplitude  $\epsilon$  is in perfect agreement with old studies on laser phase locking.<sup>14</sup>

For completeness, the linear stability analysis of Eqs.

(A1) close to the locking threshold has also been performed. The characteristic equation is a second-order one of the type  $\lambda^2 + b\lambda + c = 0$ . The critical value  $c = 0$  (condition for a tangent bifurcation) separates the stable ( $c < 0$ ) from the unstable ( $c > 0$ ) branch. On the other hand, a positive  $c$  is the requirement for complex eigenvalues so that no Hopf bifurcations can influence the stable branch and the locking threshold remains fixed at  $(I_V, A_V)$  for any parameter choice.

## APPENDIX B

Here we briefly describe the numerical method used for the computation of the periodic solutions. The approach is based on a standard Newton's method on the Poincaré section defined by the zero crossing of the field imaginary part  $y$ .

We first notice that in order to avoid stiffness problems on the phase, we have integrated the flow (3.1) in Cartesian coordinates [see Eqs. (4.5)]. Moreover, in order to get the best possible accuracy on the determination of the Poincaré section, we have followed the method outlined by Henon,<sup>15</sup> which is based on the exchange of roles between  $y$  and the time  $t$ : The former variable is transformed into the independent one, while  $t$  becomes a dependent variable.

In the following we will refer for simplicity to a generic three-dimensional flow in a space  $(x, y, z)$ , with the Poincaré section determined by the condition  $y = 0$ . The dynamical behavior is then described by a two-dimensional recursive relation from  $(x, z)$  to  $(x', z')$ ,

$$\begin{aligned} x' &= F(x, z), \\ z' &= G(x, z). \end{aligned} \quad (\text{B1})$$

The study of periodic solutions can be transformed into the quest for the zeros of a two-variable function, namely (for period-one trajectories),

$$\begin{aligned} 0 &= x_0 - F(x_0, z_0), \\ 0 &= z_0 - G(x_0, z_0). \end{aligned} \quad (\text{B2})$$

A straightforward application of Newton's method leads to the linear problem

$$x' - x = \left[ \frac{\partial F}{\partial x} - 1 \right] \delta x + \frac{\partial F}{\partial y} \delta y, \quad (\text{B3})$$

$$y' - y = \frac{\partial G}{\partial x} \delta x + \left[ \frac{\partial G}{\partial y} - 1 \right] \delta y,$$

where  $\delta x$  and  $\delta y$  are the corrections to the initial trial values  $x$  and  $y$ , respectively. We now have to evaluate all the derivatives by exploiting the flow equations. The recursive map (B1) is, in principle, determined by the conditions

$$\begin{aligned} x' &= X(T, x, z), \\ z' &= Z(T, x, z), \\ 0 &= y' = Y(T, x, z), \end{aligned} \quad (\text{B4})$$

where the third relation provides an indirect estimate for the return time  $T$  which, in general, depends on the starting point on the surface of the section. Now, taking the derivative of Eqs. (B4) we obtain the requested relations. Referring for instance to  $\partial F/\partial x$ , we have

$$\frac{\partial F}{\partial x} = \frac{\partial X}{\partial x} + \dot{X}(T) \frac{\partial T}{\partial x}, \quad (\text{B5})$$

where  $\partial T/\partial x$  is evaluated from the third of Eqs. (B4)

$$0 = \frac{\partial Y}{\partial x} + Y(T) \frac{\partial T}{\partial x}. \quad (\text{B6})$$

As a consequence, integrating three linearly independent vectors of the tangent flow, we are able to collect the whole information needed to apply Newton's method. Incidentally, we notice that, as a by-product of this procedure, the stability of the periodic solutions (related to the derivatives of  $F$  and  $G$ ) is straightforwardly evaluated.

\*Present address: Department of Chemistry, University of Toronto, Toronto, Ontario M5S 1A1, Canada.

†Present address: Department of Physics, Bryn Mawr College, Bryn Mawr, PA 19010.

‡Also with Dipartimento di Fisica, Università di Firenze, Firenze, Italy.

<sup>1</sup>N. Minorski, *Nonlinear Oscillations* (Princeton University, Princeton, NJ, 1962).

<sup>2</sup>(a) F. T. Arecchi, G. L. Lippi, G. P. Puccioni, and J. Tredicce, *Opt. Commun.* **51**, 308 (1984); and in *Coherence in Quantum Optics V*, edited by L. Mandel and E. Wolf (Plenum, New York, 1984), p. 1227; (b) J. R. Tredicce, F. T. Arecchi, G. L. Lippi, and G. P. Puccioni, *J. Opt. Soc. Am. B* **2**, 173 (1985).

<sup>3</sup>G. Iooss and D. D. Joseph, *Elementary Stability and Bifurcation Theory* (Springer, New York, 1980).

<sup>4</sup>J. Guckenheimer and P. Holmes, *Nonlinear Oscillations, Dynamical Systems, and Bifurcations of Vector Fields*, Vol. 42 of *Applied Mathematical Science* (Springer, New York, 1983).

<sup>5</sup>G. L. Oppo and A. Politi, *Europhys. Lett.* **1**, 549 (1986).

<sup>6</sup>H. Haken, *Advanced Synergetics* (Springer, Berlin, 1983).

<sup>7</sup>E. Brun, B. Derighetti, D. Meier, R. Holzner, and M. Ravani, *J. Opt. Soc. Am. B* **2**, 156 (1985).

<sup>8</sup>A. Politi, G. L. Oppo, and R. Badii, *Phys. Rev. A* **33**, 4055 (1986).

<sup>9</sup>G. L. Oppo and A. Politi, *Z. Phys. B* **59**, 111 (1985).

<sup>10</sup>The lack of stability of the branches corresponding to  $\eta=2, 2.5$ , and 3 is due to the condition (4.13) which states the existence of an unstable eigenvalue near the Hopf bifurcation for  $\eta < D$ .

<sup>11</sup>Y. Gu, D. K. Bandy, J. M. Yuan, and L. M. Narducci, *Phys. Rev. A* **31**, 354 (1985).

<sup>12</sup>M. B. Spencer and W. E. Lamb, Jr., *Phys. Rev. A* **5**, 884 (1972).

<sup>13</sup>T. Yamada and R. Graham, *Phys. Rev. Lett.* **45**, 1322 (1980).

<sup>14</sup>H. Haken, H. Sauermann, Ch. Schmid, and H. D. Vollmer, *Z. Phys.* **206**, 369 (1967); W. E. Lamb, Jr., *Phys. Rev. A* **1429**, (1964).

<sup>15</sup>M. Henon, *Physica* **5D**, 412 (1982).